

Intelligent Detection System for Electrical Equipment based on Deep Learning and Infrared Image Processing Technology

Mingxu Lu¹, Yuan Xie²

College of Artificial Intelligence Applications, Shanghai Urban Construction Vocational College, Shanghai, 201415, China¹
Library, Shanghai Construction Engineering School, Shanghai, 200241, China²

Abstract—The demand for the reliability of power grid systems is gradually increasing with the development of the power industry. And it is necessary to promptly identify and eliminate the hidden dangers. To meet the needs of online monitoring and the early warning of electrical equipment, an intelligent detection system based on deep learning and infrared image processing technology is proposed in this study. Firstly, the infrared image is preprocessed for noise reduction. Then, an improved SSD (Single Shot MultiBox Detector) network is used to optimize the infrared image detection method. Based on this, an intelligent detection system for electrical equipment is designed. The results show that the mAP value of the improved SSD network after 1200 iterations is about 92.58%, and its area under the Precision Recall (PR) curve is higher than other algorithms. The simulation analysis results of the detection system show that the improved method detects a fault degree of 57.85%, which is closer to the 59.74% in the real situation. The experimental results indicate that the newly established intelligent detection system for electrical equipment can effectively detect its abnormal situations.

Keywords—Deep learning; infrared images; electrical equipment; intelligent detection; adaptive median filtering

I. INTRODUCTION

With the rapid development of the power industry, the requirements for the reliability of the power grid system are becoming increasingly high. Equipment fault detection is a key to intelligent detection for electrical equipment. Electrical equipment faults have randomness, periodicity, concealment, and multiple occurrences, requiring constant attention to the status of electrical equipment [1-2]. Online monitoring and security warning have become important functional requirements for the power grid system. However, in order to timely identify problems and eliminate hidden dangers, a large amount of manpower and objects need to be consumed, so the intelligence and automation of the power grid are gradually being put on the agenda. The infrared image detection method is a very effective online monitoring method. It can not only detect defects through online detection, but also be combined with other methods. It can locate the fault and bring great convenience to maintenance [3]. In recent years, deep learning technology has made rapid progress. And more and more image recognition tasks have achieved good performance in deep learning solutions. It is increasingly applied to various industries, greatly promoting industry reform and innovation. Image processing, as an important branch, is becoming

increasingly intelligent with the promotion of neural network. Simultaneously, deep learning can improve the accuracy and efficiency of neural network image feature extraction and classification [4]. The long-term development of the power grid system has accumulated a large amount of infrared detection data, which can be applied to artificial intelligence technology. Based on image classification technology and automatic analysis and processing of electrical images, the current difficulties in manual data management can be effectively overcome, reducing on-site measurement and post maintenance workload. Therefore, achieving intelligent recognition of temperature anomalies in infrared images is a necessity for the development of power systems. Improving the efficiency of monitoring and ensuring the smooth operation of the power grid also inevitably requires the large-scale application of such automation technologies. Research has shown that deep learning techniques based on neural networks can improve the accuracy of image processing [5]. The combination of methods can improve the accuracy of equipment fault detection. However, improving the accuracy of equipment fault detection can easily lead to a decrease in the efficiency of the method. In order to meet the needs of online monitoring and early warning of electrical equipment, an intelligent detection system based on deep learning and infrared image processing technology was proposed in this study. Firstly, preprocessing such as noise reduction was performed on the infrared image. Then, an improved SSD (Single Shot MultiBox Detector) network was used to optimize the infrared image detection method. On this basis, an intelligent detection system for electrical equipment was designed. It is hoped to further improve the practical application effect of electrical equipment testing methods.

II. RELATED WORKS

The maintenance of power equipment is related to the safety of production, so it is necessary to improve the accuracy and effectiveness of equipment fault detection methods [6]. The abnormal situation detection of device can be judged using information from infrared images. In power equipment fault detection, infrared images can reflect the basic information of the equipment. Wang et al. designed an online electrical equipment fault detection method based on infrared images and developed relevant software. This method can perform state evaluation based on real-time device status, and its effectiveness has been proven in practical applications [7]. After obtaining the infrared image of the device, DL

model can classify the obtained image features for fault diagnosis and analysis [8]. In Shen et al.'s study, they used DL for feature extraction and classification after feature extraction of infrared images. The improved method can improve the accuracy of the detection method [9]. In the fault detection of power equipment, researchers have designed a fault detection method based on infrared images. And this method uses DL and infrared images for defect recognition and classification. Finally, through the combination of methods, the reduction of operation and maintenance costs was achieved, and the efficiency of fault detection was improved [10]. Siah et al. showed that DL combined with this technology can play a role in detecting abnormal situations in the examination of respiratory equipment. Based on infrared imaging technology, they can use infrared images to analyze whether there is an air leak in the respirator. This can effectively control the widespread spread of the virus and reduce the likelihood of public health crises [11].

The infrared images can effectively reflect the basic situation of the device. But during the image acquisition, the clarity of the image may be reduced due to the noise. To reduce the noise impact on image clarity, researchers used filtering algorithms for fault detection, which showed high image processing performance. The filtering algorithm can perform segmentation preprocessing on the collected images, thereby improving the quality of the detected image. In the study by Jayanthi et al., the improved filtering algorithm can improve the quality of collected images for tumor detection. The results confirm that the new method can assist in tumor detection and improve the accuracy of patient diagnosis [12]. The combination of median filtering and clustering algorithm can realize the image super pixel segmentation. This method can reduce noise impact and improve the quality of infrared image acquisition. Infrared images can effectively reflect the abnormal situation of device after segmentation [13]. In relevant research, filtering algorithms can significantly reduce noise impact after being weighted. And this method combines mean algorithm, which effectively protects the details of the image, improves the information processing ability and the detection performance of the image [14]. To obtain more fault information, Zhang et al. proposed the introduction of DL technology to improve filtering algorithm. This new method can mine more time-related data information. In fault recognition simulation experiments, this method can effectively extract fault features and perform accurate classification [15]. In DL, Single Shot MultiBox Detector (SSD) is a high-precision algorithm that can be used for image information processing. After continuous method improvements, Leng et al. were able to fuse features from different levels during the image sampling process. At the same time, the uniform generation of image anchors improves the accuracy of detection while ensuring the efficiency [16]. In the study by Zhou et al., SSD can use residual networks for image feature extraction when detecting sample targets. This method exhibits stronger target detection ability and higher detection accuracy in performance comparison [17].

In the above research, infrared images, filtering algorithms, and SSD have shown good performance in object detection, image processing, and feature extraction. And the combination

of methods improves the equipment fault detection accuracy. However, improving equipment fault detection accuracy can easily lead to a decrease in the efficiency of the method. To improve this situation, after preprocessing the infrared image, the improved SSD was used for image processing. It is hoped to further improve the practical application effect of electrical equipment testing methods.

III. INTELLIGENT DETECTION SYSTEM FOR ELECTRICAL EQUIPMENT BASED ON DL AND INFRARED IMAGE PROCESSING TECHNOLOGY

A. Construction of an Intelligent Detection System for Electrical Equipment and Research on Infrared Image Preprocessing

To ensure the long-term stable operation of electrical equipment detection system, system design should follow the principles of safety, adaptability, practicality, maintainability, and scalability. The framework of detection system is Django, which mainly includes the model, template, and view layer. Business logic is one important core in this framework, including infrastructure, application, model layer, etc. According to the actual needs of electrical equipment testing, this system is divided into four management modules: infrared image recognition, inspection tasks, image management, and personnel management in Fig. 1.

Infrared image recognition is the core part of the detection system, which requires preprocessing of infrared images to achieve functions such as temperature extraction, device recognition, and anomaly detection. Periodic inspections are required in inspection tasks management, as well as re-inspection and timely warning of any abnormal equipment. In image data management module, personnel can transmit image samples and view the running status and related data. The permission management of staff is the main function of the personnel management module, which can view the basic data information of relevant personnel.

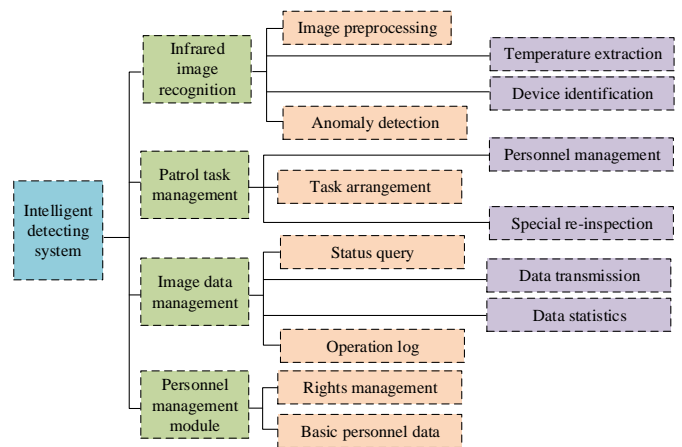


Fig. 1. Functional architecture of electrical equipment intelligent detection system.

In Fig. 2, the infrared image recognition module mainly includes image reading, image preprocessing, temperature extraction of electrical equipment, infrared image segmentation, and electrical equipment recognition. In this

study, the infrared image recognition module focuses on the noise processing of electrical equipment infrared images, as well as extraction and classification of image features. In response to the issue of infrared images being susceptible to factors such as noise, a series of processing measures were carried out. It has improved the research content of the infrared image recognition module in the intelligent detection system of electrical equipment.

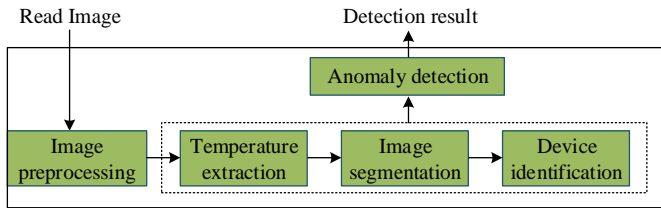


Fig. 2. Infrared image recognition module.

Noise characteristic analysis is one of the main characteristics of infrared image characteristics, and image noise has a certain degree of randomness and regularity. Noise has a significant impact on the detection of electrical equipment images, mainly including background noise, detector noise and amplifier noise, etc. The infrared image can be denoised by using Gaussian filter, mean filter, median filter, and other methods. The median filter can calculate the results in linear time. This method is simple in calculation and can perform fast filtering processing. The noise processing process of median filter algorithm includes the following contents. First, all pixel values in the neighborhood of pixel to be processed are arranged into a sequence according to the size of the pixel value. The pixel value at the interval position is the desired median. Then, the pixel values that need to be processed are replaced with median values to improve the closeness between the neighboring pixel values and the true values in Fig. 3.

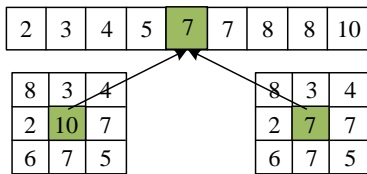


Fig. 3. Schematic diagram of the principle of median filtering.

In the median filtering algorithm, a window is defined that it is mostly odd with a length of $L = 2N + 1$, and N is a positive integer. The sample signal $\{X(i - N), \dots, X(i), \dots, X(i + N)\}$ can be obtained. Formula (1) is the output value of the median filter.

$$Y(i) = MED\{X(i - N), \dots, X(i), \dots, X(i + N)\}, i \in Z \quad (1)$$

In formula (1), $X(i)$ is the value of window center signal sample, $N = (L - 1) / 2$, and Z represents the set of integers. The median filtering template is larger, the noise removal effect is better, but the clarity of the infrared image decreases. To effectively remove noise and ensure the details in infrared images, researchers propose an AMF. This method can automatically select template size and select the smallest

template for filtering processing when corresponding pixel value noise removing. It can simultaneously remove noise and ensure image clarity. In AMF, the window corresponding to the image pixel (x, y) during filtering is first defined as S_{xy} , and then the following two processing processes are performed. The first step is the processing of the first layer in formula (2).

$$Z_{A1} = Z_{med} - Z_{min}, Z_{A2} = Z_{max} - Z_{med} \quad (2)$$

In formula (2), Z_{min} , Z_{med} , and Z_{max} represents the minimum, median, and maximum values of pixel grayscale in window S_{xy} , respectively. If $Z_{A1} > 0$ and $Z_{A2} < 0$, it needs to be transferred to the second algorithm layer. On the contrary, it is necessary to increase the size of window S_{xy} . If the size is less than or equal to the maximum window size allowed by S_{xy} , then the processing of the first layer needs to be repeated. Otherwise Z_{med} will be output. Formula (3) is the processing method for the second layer.

$$Z_{B1} = Z_{xy} - Z_{min}, Z_{B2} = Z_{max} - Z_{xy} \quad (3)$$

In formula (3), Z_{xy} is the grayscale value at pixel point (x, y) . If $Z_{B1} > 0$ and $Z_{B2} < 0$, the current Z_{xy} is output, otherwise Z_{med} is output. AMF can be used to filter out salt and pepper noise. During image processing, it needs to preserve image details as much as possible while removing noise. After denoising, infrared images become blurry, making it difficult for subsequent feature extraction and recognition. Therefore, image enhancement processing is also required after denoising [18]. The grayscale histogram of infrared images can provide information such as the overall contrast, average brightness, and dynamic range of image pixel values. To enhance the clarity of infrared image gray histogram, piecewise linear transformation, gamma correction and histogram equalization can be used to enhance the clarity of image details. In this experiment, the adaptive histogram equalization method is selected for image enhancement. The main improvements of this method in image processing include two points. Firstly, the grayscale threshold of the histogram is set, and the parts exceeding the threshold are cropped. And it is evenly divided into various gray levels to avoid excessive enhancement of noise points. Secondly, interpolation methods are used to accelerate the equalization of grayscale histograms. After the equalization of adaptive histogram, the gray histogram of infrared image can enhance image contrast without obvious noise enhancement.

B. Intelligent Detection Algorithm based on DL and Infrared Images

After preprocessing the infrared image, it is necessary to extract and classify the image features. SSD can classify the feature maps of the infrared image according to their size for target detection at various scales. When conducting intelligent detection of electrical equipment, the first step is to input the infrared image of the electrical equipment. After the feature extraction through convolutional layers, feature maps with different scales are generated. Then, prior boxes of different

scales are generated on these special maps with different scales, and the predicted target boundary boxes are detected and classified. On this basis, redundant detection boxes are suppressed and deleted, and finally detection results are

generated. The method of suppressing detection boxes is processed using non-maximum values. Fig. 4 shows the flowchart of the SSD algorithm.

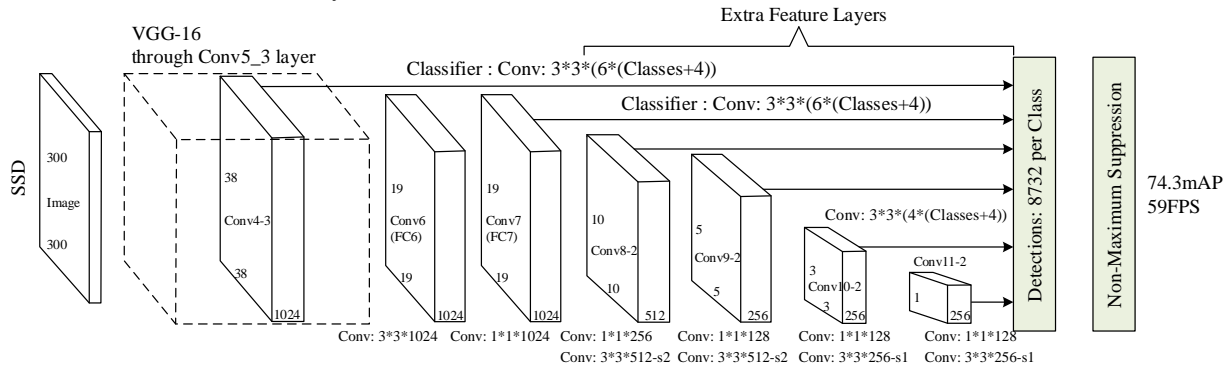


Fig. 4. Flowchart of SSD.

The length and width of prior boxes number and prior boxes in SSD need to be set in advance. These parameters can significantly affect the efficiency and accuracy of algorithm [19]. In response to the characteristics of electrical equipment fault detection, appropriate prior boxes need to be set, so SSD can be improved. The improved SSD first utilizes the K-means algorithm to iteratively analyze data targets and find the optimal number of prior boxes. Due to the fact that Euclidean distance is a commonly used method in K-means, this method can increase the computational error of the larger prior boxes. The intersection over union (IOU) of two prior boxes is selected as the standard for method judgment in formula (4).

$$IOU = \frac{Detection \quad Result \cap Ground \quad Truth}{Detection \quad Result \cup Ground \quad Truth} \quad (4)$$

In formula (5), *Detection Result* is the predicted bounding box and *Ground Truth* represents the true bounding box. IOU value reflects the proximity between the predicted bounding box and the true bounding box, which is proportional to each other. Formula (5) is the Euclidean distance calculation based on IOU as the standard.

$$d(box, centriod) = 1 - IOU(box, centriod) \quad (5)$$

In formula (5), *box* is the prior box and *truth* represents the true box. Formula (6) is the objective function of K-means.

$$S = \min \sum_{i=1}^k [1 - IOU(box - truth)] \quad (6)$$

When $k=4$, the clustering objective function remains basically stable, so the number of prior boxes is set to 4. After determining the setting of prior box parameters, improvements are made to the basic network. VGG-16 is used for extracting features, which has high testing accuracy but high computational complexity. To reduce the computational difficulty and improve the computational speed, researchers proposed the MoblieNet network structure [20]. MoblieNet

network can convert ordinary convolutions into a combination of deep convolutions and point convolutions using deep separable convolutions. Formula (7) is the calculation of deep separable convolutions.

$$F \times F \times D \times N \times N + 1 \times 1 \times D \times K \times N \times N \quad (7)$$

In formula (7), F means convolution kernel dimension, D is input depth, N refers to input width and height, and K represents output depth. By comparing deep separable convolutions computational complexity with that of standard convolutional networks, the comparison result representation method in formula (8) can be obtained.

$$\frac{F \times F \times D \times N \times N + 1 \times 1 \times D \times K \times N \times N}{F \times F \times N \times N \times D \times K} = \frac{1}{K} + \frac{1}{F^2} \quad (8)$$

If 3×3 convolutional kernel is used in the calculation, the computational difficulty can be reduced by 8-9 times. The MoblieNetV2 network structure uses 1×1 convolutional layer to expand the number of feature map channels. Then, the feature extraction of infrared images was carried out, and 3×3 deep separable convolution method is used. Next, the extracted image features were dimensionally reduced, and 1×1 convolutional layer was selected. In MoblieNet V2 network structure, the linear activation function is used at the low dimension layer, and the feature reuse structure of ResNet is introduced to improve the low dimension data collapse and the lack of reuse features in the MoblieNet V1 network. It can improve the accuracy of the algorithm and reduce latency. To make the network layer thinner, the width scaling factor α is introduced in the MoblieNet V2 network structure, which changes the depth of the input and output channels to αD and αK , respectively. In formula (9), the computational complexity of the MoblieNet V2 network can be reduced to α^2 of the original computational complexity.

$$F \times F \times \alpha D \times N \times N + 1 \times 1 \times \alpha D \times \alpha K \times N \times N \quad (9)$$

MoblieNet V2 network structure optimizes the network structure and activation function on the basis of MoblieNet V1. While improving testing accuracy, it can also save more feature information, reducing computational difficulty.

Therefore, in this experiment, the VGG-16 basic network of the SSD algorithm will be replaced with the MoblieNet V2 network structure. The improved SSD algorithm is developed to improve the algorithm's computational speed and testing accuracy.

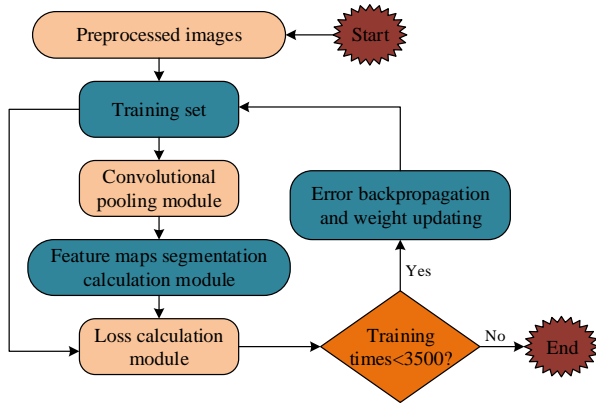


Fig. 5. Training flowchart of improved SSD algorithm.

Fig. 5 shows the training flowchart of the improved SSD algorithm. When algorithm training, the loss function uses the weighted sum of the position error loc and the confidence error $conf$ of SSD in formula (10).

$$L(x, c, l, g) = \frac{1}{N} (L_{conf}(x, c) + \alpha L_{loc}(x, l, g)) \quad (10)$$

In formula (10), N means positive samples number, c represents the confidence value of the predicted category, l stand for the position of the predicted corresponding bounding box, g represents the position parameter of the true bounding box, and α refers to the weight coefficient. For loc , the $smooth_{L1}$ loss function in formula (11) is used.

$$smooth_{L1}(x) = \begin{cases} 0.5x^2 & |x| < 1 \\ |x| - 0.5 & otherwise \end{cases} \quad (11)$$

From this, the calculation of L_{loc} in formula (12) can be obtained.

$$L_{loc}(x, l, g) = \sum_{i \in Pos} \sum_{m \in \{cx, cy, w, h\}} x_{ij}^k \cdot smooth_{L1}(l_i^m - \hat{g}_j^m) \quad (12)$$

In formula (12), cx, cy are the center coordinates of the positioning box, w, h are the width and height of the positioning box, and \hat{g} is the value obtained after encoding. Formula (13) is the encoding method for central coordinate.

$$\begin{cases} \hat{g}_j^{cx} = (g_j^{cx} - d_i^{cx}) / d_i^w / variance[0] \\ \hat{g}_j^{cy} = (g_j^{cy} - d_i^{cy}) / d_i^h / variance[1] \end{cases} \quad (13)$$

In formula (13), d represents the prior box position, and

$variance$ is hyperparameter, and \hat{g} can be scaled. Formula (14) is the encoding method for width and height.

$$\begin{cases} \hat{g}_j^w = \log(g_j^w / d_i^w) / variance[2] \\ \hat{g}_j^h = \log(g_j^h / d_i^h) / variance[3] \end{cases} \quad (14)$$

For $conf$, the softmax loss function in formula (15) is used.

$$L_{conf}(x, c) = - \sum_{i \in Pos} x_{ij}^p \log(\hat{c}_i^p) - \sum_{i \in Neg} \log(\hat{c}_i^0) \quad (15)$$

In formula (15), $x_{ij}^p \in \{1, 0\}$, which represents the parameter indicator. $x_{ij}^p = 1$ means that the predicted boundary box i is in a state of coincidence with the actual boundary box j . At this point, the category is p , and the higher the probability prediction, the smaller the loss. Therefore, the probability passes and softmax is generated.

IV. EXPERIMENTAL RESULTS AND ANALYSIS

A. Performance Verification Experiment of Intelligent Detection Algorithm

AMF can effectively reduce the interference of salt and pepper noise, and the processed infrared image quality can be improved with less external influence, making the process more convenient and faster. The denoising performance of AMF is compared with that of Gaussian filter, mean filter, and median filter algorithm. Signal to Noise Ratio (SNR), Peak Signal to Noise Ratio (PSNR) and Mean Square Error (MSE) are selected as performance comparison indicators. SNR and PSNR are larger, as well as MSE is smaller, algorithm's denoising effect is better. The deep learning framework is Tensorflow-1.13.0rc2. During network training, the initial learning rate is set to 0.0001, the beam size is 16, the encoding scaling factor variable = [0.1 0.1 0.1 0.2 0.2], and the weight coefficient of the loss function is $\alpha=0.2$. The results are shown in Table I.

From Table I, the SNR and PSNR of AMF are greater than those of Gaussian filter, mean filter, and median filter algorithms under different noise concentrations. The MSE of AMF is less than that of Gaussian filter, mean filter, and median filter algorithms. The performance comparison results of different noise processing methods show that AMF is better than Gaussian filter, mean filter, and median filter algorithms in infrared image noise processing.

In Fig. 6, the filtered images of different methods were compared when the noise concentration was 0.02. From the figure, AMF has a higher clarity of the filtered image and better similarity to the original image. Compared to other image processing methods, AMF exhibits better image processing performance. This method can effectively handle the impact of noise and has better denoising effect.

TABLE I. RESULTS OF DIFFERENT NOISE TREATMENT METHODS

Noise concentration	Mean filtering algorithm			Median filter algorithm		
	SNR/dB	PSNR/dB	MSE	SNR/dB	PSNR/dB	MSE
0.01	50.05	52.68	0.004	52.68	58.95	0.003
0.02	43.52	51.63	0.006	49.21	57.89	0.004
0.03	41.18	49.29	0.007	45.26	55.37	0.005
0.04	36.51	44.74	0.008	43.26	51.77	0.008
0.05	31.14	39.32	0.014	42.25	51.03	0.013
0.06	22.49	30.58	0.036	37.52	46.15	0.034
0.07	15.94	24.02	0.071	36.41	44.98	0.067
Noise concentration	Gaussian filter algorithm			AMF		
	SNR/dB	PSNR/dB	MSE	SNR/dB	PSNR/dB	MSE
0.01	53.7336	56.559	0.003	55.31	61.90	0.002
0.02	46.7262	55.437	0.004	51.67	60.78	0.003
0.03	44.217	52.9176	0.006	47.52	58.14	0.004
0.04	39.1986	48.0318	0.007	45.42	54.36	0.005
0.05	33.4356	42.2178	0.008	44.36	53.58	0.006
0.06	24.1434	32.8338	0.011	39.40	48.46	0.009
0.07	17.1156	25.7856	0.023	38.23	47.23	0.011

Mean average precision (mAP) can be used to evaluate the performance of network models. In the performance research of the intelligent detection algorithms based on DL and infrared images, mAP was used to evaluate the performance. Fig. 7 shows the mAP curve in validation set. From Fig. 7, as the number of training sessions increases, the mAP value of the proposed model continues to increase. In 0-1200 iterations,

the mAP value changes the most significantly and the accuracy increases significantly, indicating that the model is still in the learning stage in the 0-1200 iterations. When iterations exceed 1200, the mAP value gradually stabilizes and the curve gradually converges. After the model was trained in the validation set, its average accuracy was tested in the test set, and the final mAP value measured was 92.58%.

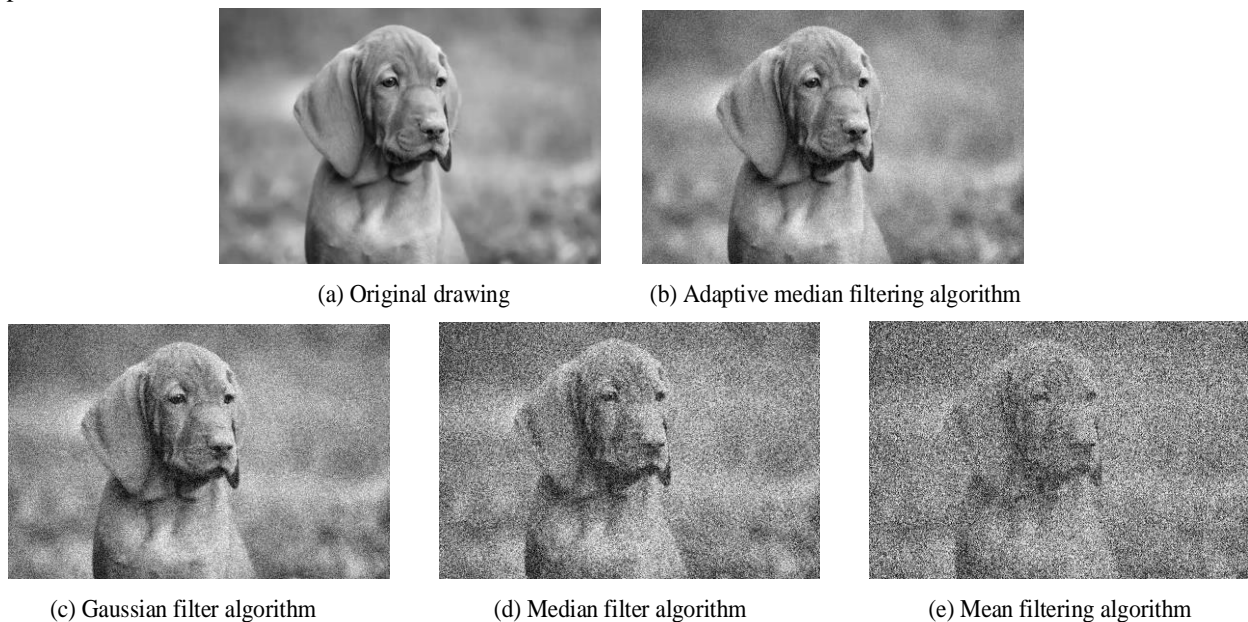


Fig. 6. Filter images of different algorithms.

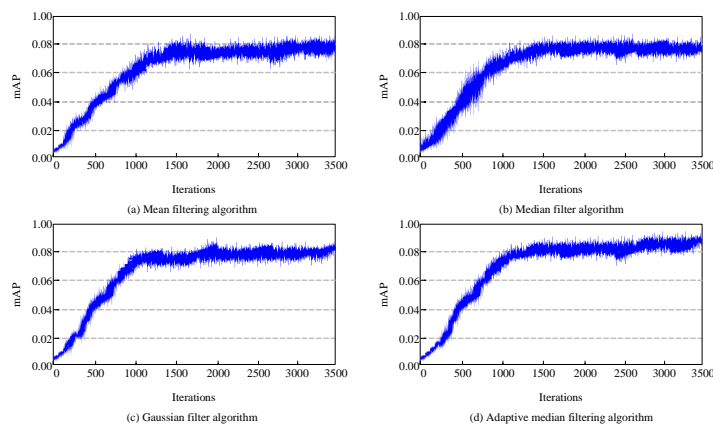


Fig. 7. mAP curve.

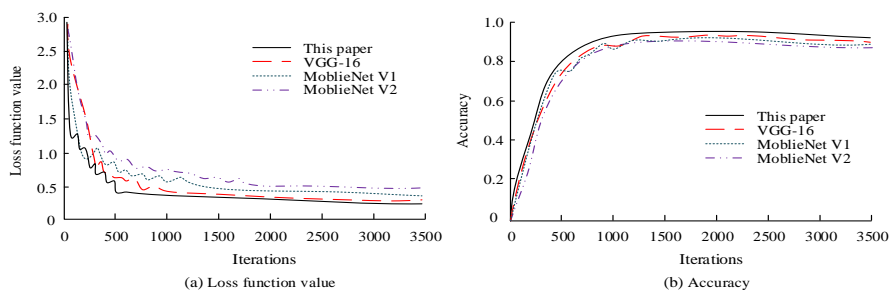


Fig. 8. Change of loss function value and quasi curvature.

The loss function can be used to describe the convergence degree of algorithm, and the accuracy can reflect algorithm precision. Therefore, this study will compare the performance of the proposed algorithm with VGG-16, MoblieNet V1, and MoblieNet V2 in Fig. 8. The algorithm in this paper tends to be stable after 500 iterations and reaches the convergence state. Its final loss function value is 0.31. Its accuracy stabilized after 950 iterations, and its final accuracy was 92%. Compared to VGG-16, MoblieNet V1, and MoblieNet V2, this algorithm has higher convergence speed and accuracy.

MoblieNet V1, and MoblieNet V2. The results are shown in Fig. 9. From Fig. 9, the area under PR curve of the proposed algorithm is higher than that of VGG-16, MoblieNet V1, and MoblieNet V2 algorithms, proving that the optimized SSD algorithm has good accuracy. The image feature extraction accuracy in improved algorithm is good, and the running time is shortened, which has good detection and classification performance.

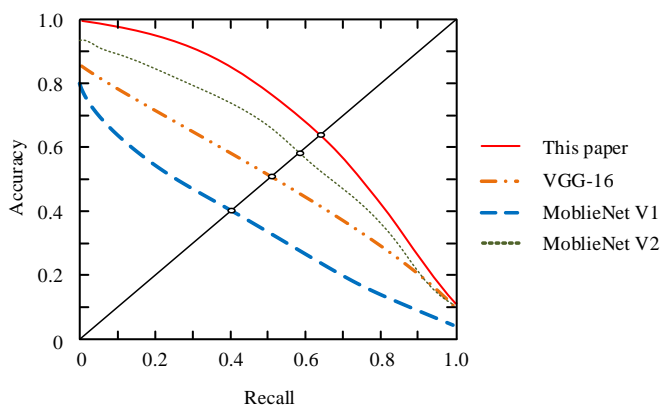


Fig. 9. Comparison of PR curves.

Precision (P) and Recall (R) are used to describe sample classification accuracy and have many applications in evaluating model performance. The Precision Recall (PR) curve is a comprehensive judgment of P and R. This study compared performance of our algorithm with VGG-16,

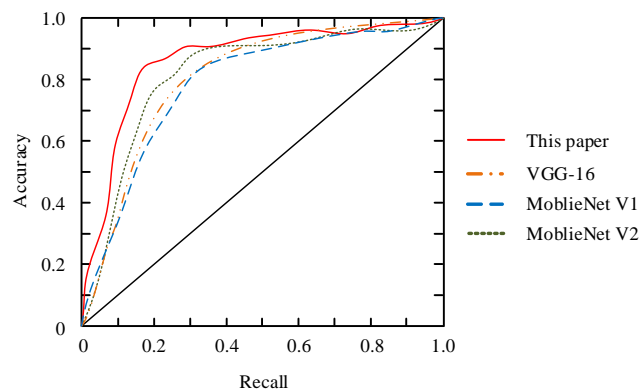


Fig. 10. Comparison of ROC curves.

In Fig. 10, the receiver operating characteristic curve (ROC) of different algorithms was simultaneously verified. From the figure, the area under ROC curve of the algorithm proposed in this experiment is the largest, and the validation results of ROC curve are consistent with those of PR curve. Based on the above performance analysis results, the algorithm proposed in this experiment has high accuracy, short running time, and good performance.

B. Simulation Analysis of Intelligent Detection System for Electrical Equipment

Circuit breakers in electrical equipment may be damaged if they are out of oil or in other abnormal conditions. In severe cases, explosions may occur and intelligent detection of circuit breakers is necessary. In the simulation analysis of the intelligent detection system for electrical equipment, the experiment selected the fault detection of circuit breakers for example analysis. Firstly, pre-processing such as noise reduction and image enhancement was performed on the collected infrared of the circuit breaker. Then, an improved algorithm was used for graphic feature extraction and classification. By comparing abnormal and normal images, the abnormal condition of the circuit breaker was analyzed and judged. To verify the superiority of the intelligent detection method for electrical equipment based on deep learning and infrared processing technology, the threshold method, region method, clustering method, and the methods in this experiment were compared for anomaly detection of circuit breakers. The results are shown in Fig. 11.

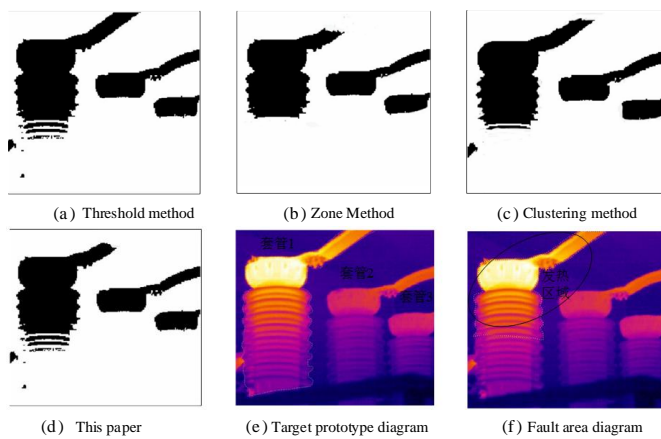


Fig. 11. Comparison of infrared image analysis of circuit breakers.

From Fig. 11, in the original image of the circuit breaker, there is a large heating area in sleeve 1. After the judgment and analysis, the contact of sleeve 1 has a heating situation, and there is also a problem of poor contact, resulting in abnormal heating of the sleeve. After comparing four detection methods, it can be seen that the improved infrared image is closer to the real image. At the same time, the fault degree of various detection methods was compared. The improved method detected a fault degree of 57.85%, which is closer to the 59.74% in the real situation. Its fault detection accuracy is higher. The intelligent detection system established in this experiment can be better applied to the fault detection of electrical equipment. In order to verify the effectiveness of the proposed method in detecting fault states, comparative experiments were conducted on a test set for 20 types of faults. At the same time, the fault detection rates of different detection methods [21-22] were compared, as shown in Table II. The best detection results for each type of fault in the table are highlighted in bold. The experimental results show that the proposed method achieved the best results 14 times, which is higher than other methods. At the same time, the proposed method has a detection rate of more than 10% higher than other methods for faults 16 and 19. The above

simulation results confirm that the proposed method exhibits high detection performance in electrical equipment fault detection.

TABLE II. RESULTS OF FAULT DETECTION RATES

Fault type	Reference 21	Reference 22	Reference 23	This paper
Fault 1	99.38	99.40	94.53	100.00
Fault 2	99.25	97.61	98.51	98.75
Fault 3	28.16	67.46	92.54	56.52
Fault 4	99.50	99.50	91.54	100.00
Fault 5	34.46	99.40	92.54	91.79
Fault 6	100.00	100.00	100.00	100.00
Fault 7	100.00	100.00	100.00	100.00
Fault 8	97.51	95.32	86.57	94.41
Fault 9	34.33	64.87	31.84	70.89
Fault 10	59.20	82.88	90.55	97.01
Fault 11	76.50	86.37	82.59	90.92
Fault 12	98.63	95.22	90.55	98.14
Fault 13	84.95	91.44	89.55	97.01
Fault 14	99.50	99.50	96.52	100.00
Fault 15	34.06	65.17	32.84	52.34
Fault 16	54.97	87.26	87.56	98.26
Fault 17	94.77	92.44	91.54	94.72
Fault 18	90.05	91.24	88.56	100.00
Fault 19	41.92	75.02	45.37	87.94
Fault 20	62.07	86.37	81.59	89.68
Average value	74.46	88.82	83.26	90.92
Optimal number	6	3	3	14

V. CONCLUSION

The electrical equipment detection system requires accurate status recognition and judgment of electrical equipment to ensure the safety of production practice. In this design of the electrical equipment intelligent system, deep learning technology and infrared image processing technology are used to identify and judge the abnormal situations of electrical equipment. The experimental results of noise processing shows that the SNR and PSNR values of AMF are higher than those of Gaussian filter, mean filter and median filter algorithms. The MSE values of AMF are lower than those of other algorithms. In the research of infrared image processing, when the iterations exceed 1200, the mAP value of the improved SSD gradually stabilizes and the curve gradually converges. After this model was trained in the validation set, the improved algorithm was tested for average accuracy in test set, and the final mAP value measured was 92.58%. The area under PR curve of improved SSD algorithm is higher than that of VGG-16, MoblieNet V1, and MoblieNet V2 algorithms, demonstrating its good accuracy. In actual fault detection experiment of electrical equipment, the fault degree of various detection methods was compared. The

improved method detected a fault degree of 57.85%, which is closer to the 59.74% in real situation, and its fault detection accuracy is higher. The intelligent detection system established in this experiment can be well applied to electrical equipment fault detection. This study is based on a deep learning system for anomaly recognition of electrical equipment, which can automatically recognize infrared images of equipment captured during inspection tasks. When the equipment is abnormal, a warning message is issued to remind the staff to inspect and repair it, so that problems can be detected in a timely manner. This can prevent larger grid failures and greatly reduce economic waste and human and material resources. At present, this method is still in secondary development and testing, and has not been widely applied in the power grid. The main reasons are as follows. Firstly, most of the samples of infrared devices come from daily infrared charged detection, which has problems such as a small sample size, inconsistent format, non-standard shooting, and lack of data labeling. These issues directly constrain the improvement of diagnostic accuracy of infrared devices based on big data. Moreover, the appearance of different devices varies, which can have an impact on the adaptability and accuracy of recognition and partitioning algorithms. At present, the deep neural network used for infrared image partitioning requires a large amount of computation, mainly relying on the computing power of the backend server. From a practical application perspective, there is an urgent need for real-time diagnosis in infrared detection sites. Real time diagnosis can provide more timely equipment defect prompts for professionals, avoiding unnecessary retesting and retesting. However, due to the large amount of image information and the large number of image files, the use of background diagnosis mode requires high transmission bandwidth. They increase the burden on communication links and network backend, and also reduce the reliability of the entire diagnostic system. Therefore, further improvements are needed in future research on this detection method.

REFERENCES

- [1] Kahlen J N, Andres M, Moser A. Improving Machine-Learning Diagnostics with Model-Based Data Augmentation Showcased for a Transformer Fault. *Energies*, 2021, 14(20): 6816-6835.
- [2] Wadi M. Fault detection in power grids based on improved supervised machine learning binary classification. *Journal of Electrical Engineering*, 2021, 72(5): 315-322.
- [3] K Wang, S Yuan, Z Yao, J Gao, J Feng. Design and Implementation of Infrared Image Classification Algorithm for Defective Power Equipment Based on Deep Learning. *Nonlinear Optics, Quantum Optics*, 2022, 56(1/2): 83-95.
- [4] J Wang, J Ou, Y Fan, L Cai, M Zhou. Online Monitoring of Electrical Equipment Condition Based on Infrared Image Temperature Data Visualization. *IEEJ Transactions on Electrical and Electronic Engineering*, 2022, 17(4): 583-591.
- [5] S Tiwari, K Falahkheirkhah, G Cheng, R Bhargava. Colon Cancer Grading Using Infrared Spectroscopic Imaging-Based Deep Learning. *Applied Spectroscopy*, 2022, 76(4): 475-484.
- [6] Bindhu V, Ranganathan G. Effective Automatic Fault Detection in Transmission Lines by Hybrid Model of Authorization and Distance Calculation through Impedance Variation. *Journal of Electronics and Informatics*, 2021, 3(1):36-48.
- [7] J Wang, J Ou, Y Fan, L Cai, M Zhou. Online Monitoring of Electrical Equipment Condition Based on Infrared Image Temperature Data Visualization. *IEEJ Transactions on Electrical and Electronic Engineering*, 2022, 17(4): 583-591.
- [8] Envelope W, Xr A. Electrical Fault Detection Equipment Based on Infrared Image Fusion. *Procedia Computer Science*, 2022, 208(1): 509-515.
- [9] Shen K, Shi Q, Wang H. Multimodal Visibility Deep Learning Model Based on Visible-Infrared Image Pair. *Journal of Computer-Aided Design & Computer Graphics*, 2021, 33(6): 939-946.
- [10] K Wang, S Yuan, Z Yao, J Gao, J Feng. Design and Implementation of Infrared Image Classification Algorithm for Defective Power Equipment Based on Deep Learning. *Nonlinear Optics, Quantum Optics*, 2022, 56(1/2): 83-95.
- [11] C Siah, S Lau, S Tng, C Chua. Using infrared imaging and deep learning in fit-checking of respiratory protective devices among healthcare professionals. *Journal of nursing scholarship: an official publication of Sigma Theta Tau International Honor Society of Nursing*, 2021, 54(3): 345-354.
- [12] N Jayanthi, D Manohari, MY Sikkandar, MA Aboamer, MI Waly, C Bharatiraja. Multi-Model Detection of Lung Cancer Using Unsupervised Diffusion Classification Algorithm. *Computers, Materials and Continua (Tech Science Press)*, 2022, 31(2): 1317-1329.
- [13] Liu H, Hu J. An adaptive defect detection method for LNG storage tank insulation layer based on visual saliency. *Process Safety and Environmental Protection*, 2021, 156(1): 465-481.
- [14] Shao C, Kaur P, Kumar R. An Improved Adaptive Weighted Mean Filtering Approach for Metallographic Image Processing**. *Journal of Intelligent Systems*, 2021, 30(1): 470-478.
- [15] Zhang Y, Lv Y, Ge M. A Rolling Bearing Fault Classification Scheme Based on k-Optimized Adaptive Local Iterative Filtering and Improved Multiscale Permutation Entropy. *Entropy (Basel, Switzerland)*, 2021, 23(2): 191-213.
- [16] Leng J, Liu Y. Single-shot augmentation detector for object detection. *Neural Computing and Applications*, 2021, 33(8): 3583-3596.
- [17] F Zhou, F He, C Gui, Z Dong, M Xing. SAR target detection based on improved SSD with saliency map and residual network. *Remote Sensing*, 2022, 14(1): 180-189.
- [18] Zhang Q, Zhao L, Zhao L. A two-step robust adaptive filtering algorithm for GNSS kinematic precise point positioning. *Chinese Journal of Aeronautics*, 2021, 34(10): 210-219.
- [19] D Li, G Meng, Z Sun, L Xu. Autonomous multiple tramp materials detection in raw coal using single-shot feature fusion detector. *Applied Sciences*, 2021, 12(1): 107-113.
- [20] Wang Z, Feng J, Zhang Y. Pedestrian detection in infrared image based on depth transfer learning. *Multimedia Tools and Applications*, 2022, 81(27): 39655-39674.
- [21] Thomas J B, Shihabudheen K V. Neural architecture search algorithm to optimize deep transformer model for fault detection in electrical power distribution systems. *Engineering Applications of Artificial Intelligence*, 2023, 120: 105890.
- [22] Levin V M, Yahya A A. An innovative method of fault detection in power transformers. *International Journal of Electrical and Computer Engineering (IJECE)*, 2022, 12(2): 1123-1130.
- [23] Kullu O, Cinar E. A deep-learning-based multi-modal sensor fusion approach for detection of equipment faults[J]. *Machines*, 2022, 10(11): 1105-1121.